Particle Acceleration at Weak Shocks induced by Mergers of Galaxy Clusters

Hyesung Kang (Pusan National University, Rep. of Korea),
Dongsu Ryu, Ji-Hoon Ha, Sunjung Kim (UNIST, Rep. of Korea)

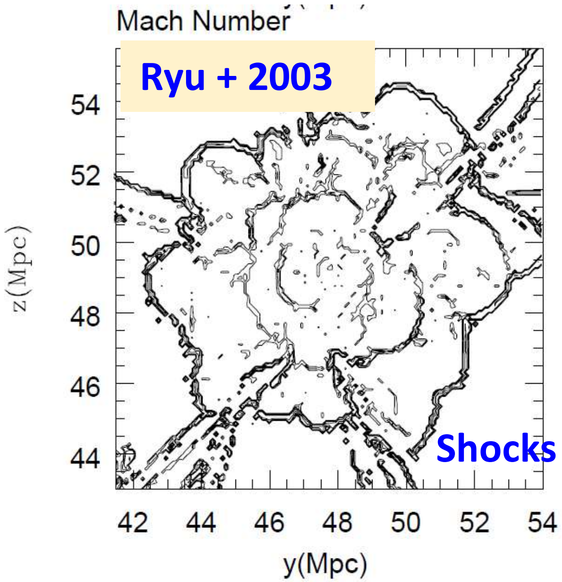

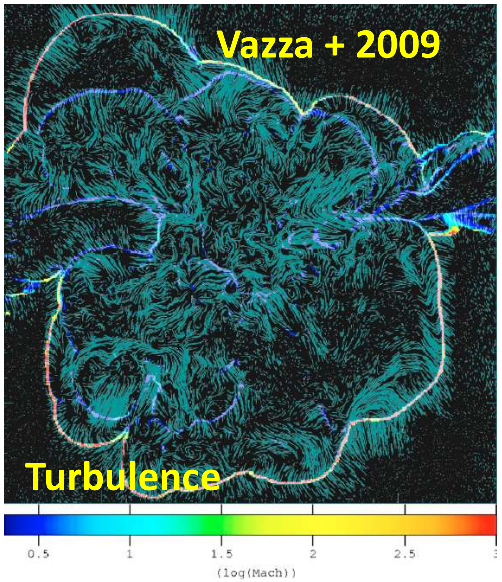

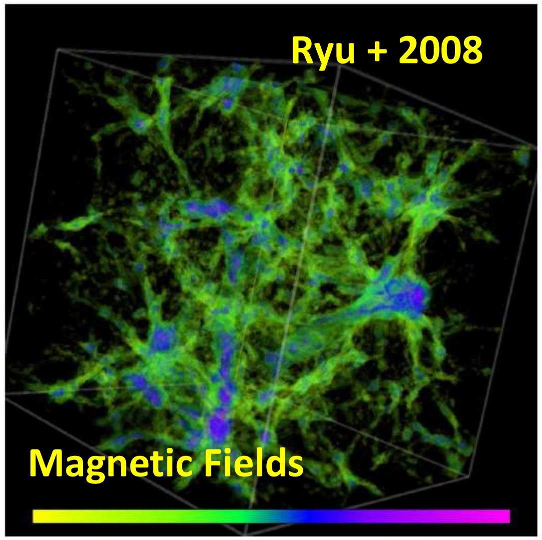

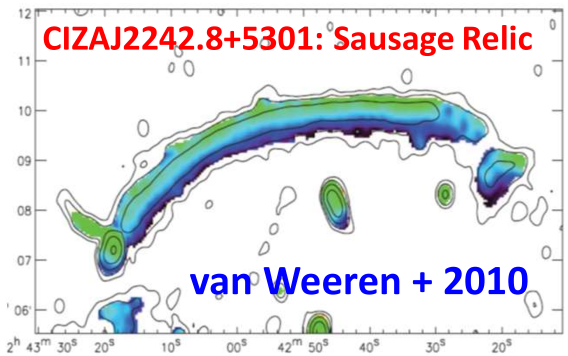

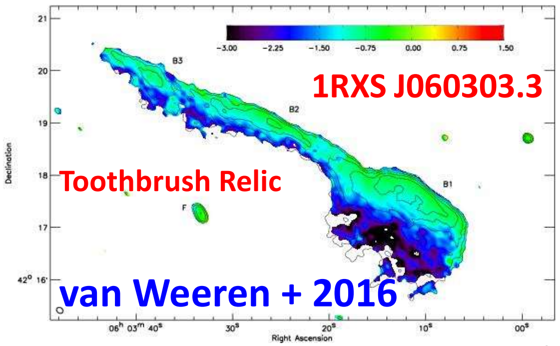

Outline

- **Shocks driven by binary mergers of galaxy clusters**
- **Observed Properties of ICM Shocks: “Radio Relic Shocks”**
- **Shock criticality: subcritical vs. supercritical**
- **Proton acceleration at Q-par high-β shocks**
- **Electron acceleration at Q-perp high-β shocks**
- **Shock re-acceleration of Fossil electrons**
- **Summary**

Binary mergers in LCDM cosmological simulations

Ha et al. 2018

X-ray emissivity Shock Mach no DM density

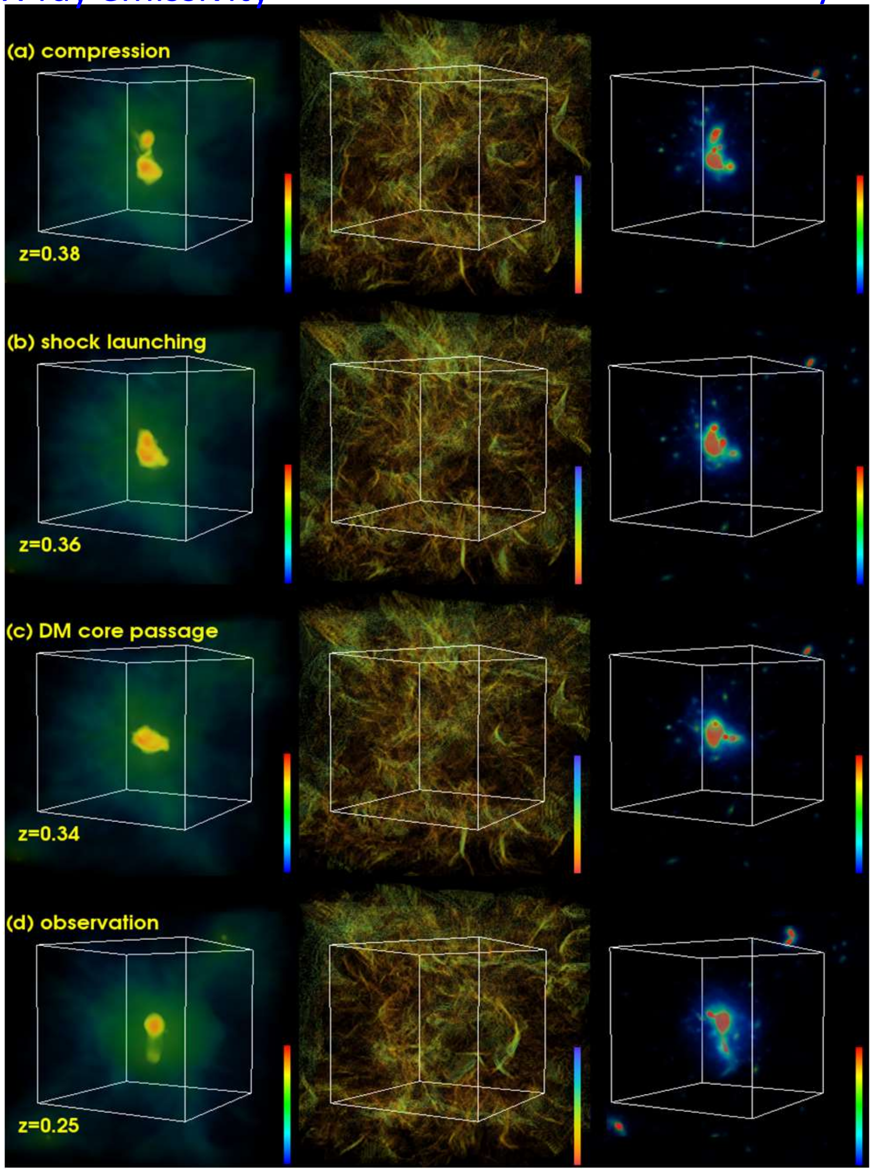

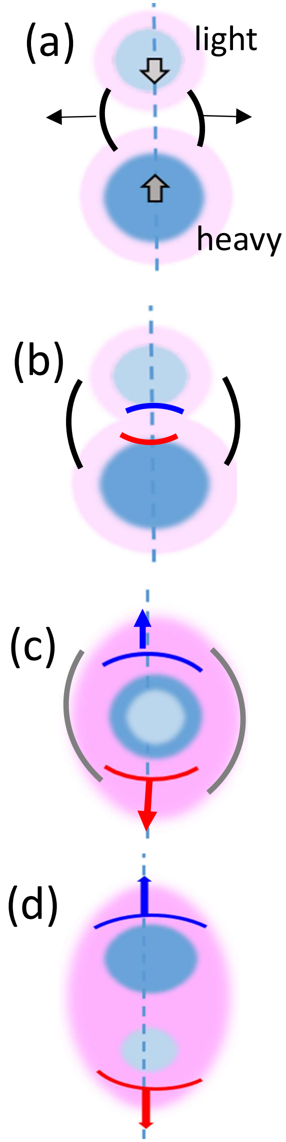

(a) During the pre-merger stage, **equatorial shocks** are lunched perpendicular to the merger axis.

(b) **Axial shocks** are lunched along the merger axis.

(c) After DM core passage, double shocks expand outward.

(d) Formation of double merger shocks (→ double radio relics)

mass ratio $m_1 : m_2$
impact factor b

typical merger shocks
- M_s ~ 1.5 - 3
- V_s ~ 1.5 -3 x10^3 km/s

Shocks are induced by supersonic flows driven by mergers of galaxy clusters

Radio Relics: Electrons accelerated at Weak $Q_\perp$ ICM Shocks

Sausage Relic

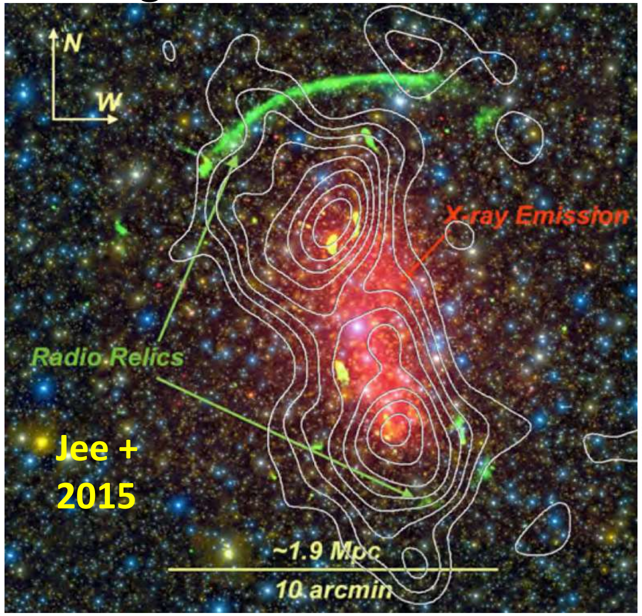

Merger geometry

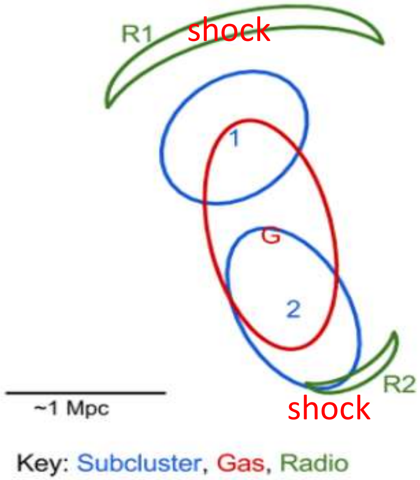

Merger of Galaxy Clusters

- ➔ Merger-driven shocks on ~1-2 Mpc scales
- ➔ Accelerate CR **electrons** via DSA
- ➔ Diffuse synchrotron radiation

Radio spectral index $M_{\rm radio}^2 = \frac{(3+2\alpha_{\rm sh})}{(2\alpha_{\rm sh}-1)}$

$$M_{\rm radio} \sim 2 - 3.0$$

DSA can explain the origin of Radio Relics in merging clusters.

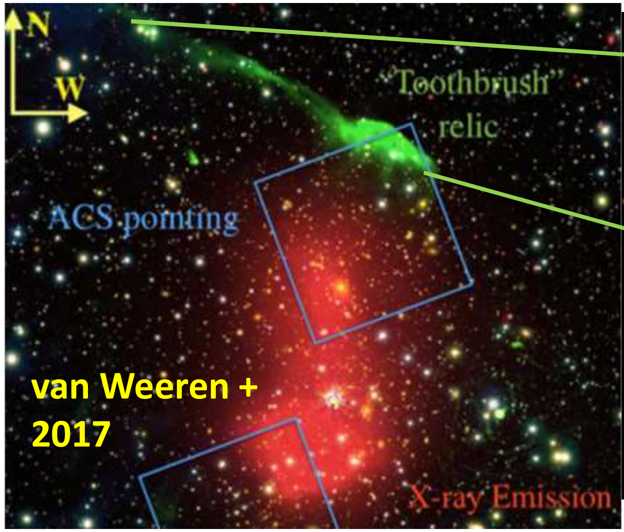

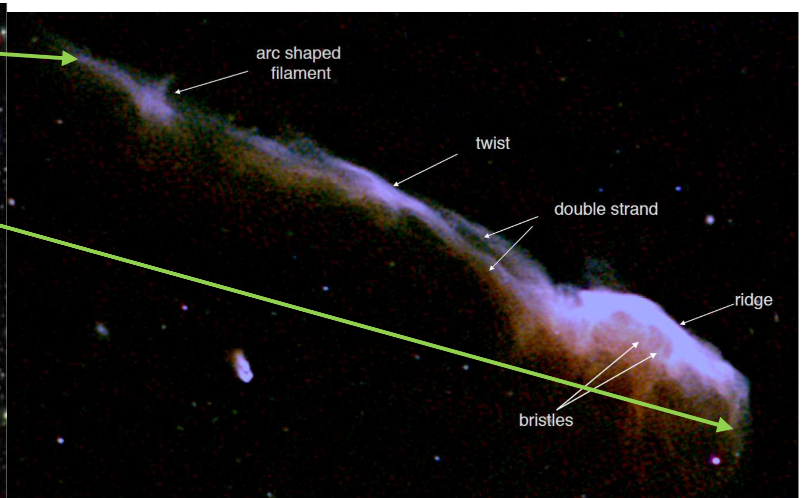

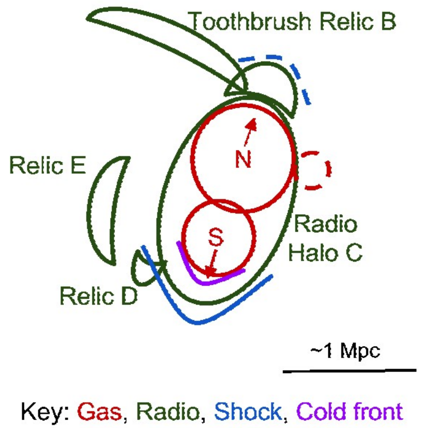

DSA = Diffusive Shock Acceleration, aka, Fermi first order process.

X-ray shocks in merging clusters

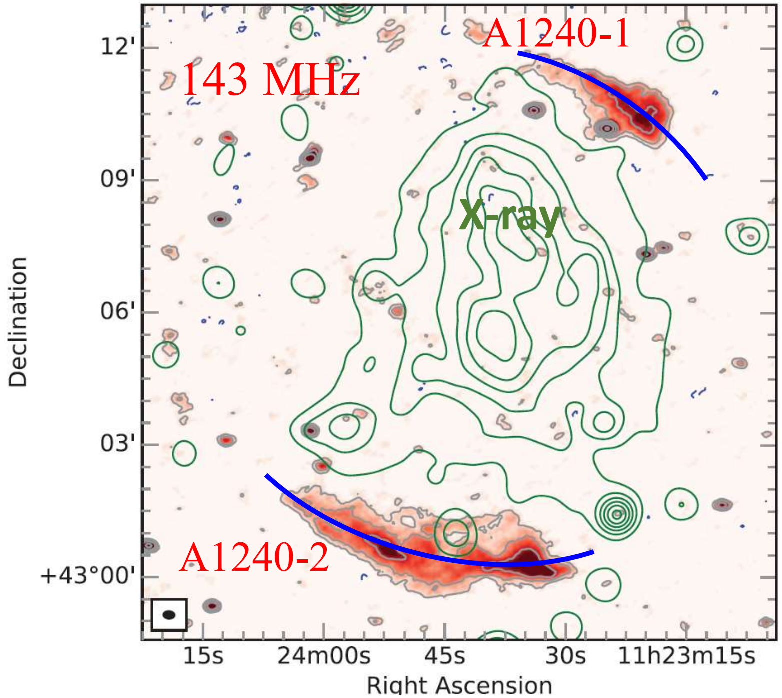

Hoang + 2018

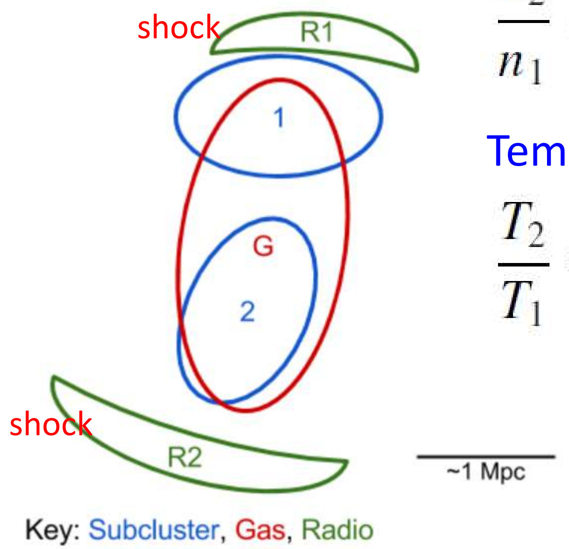

Density jump

$$\frac{n_2}{n_1} = \frac{4\mathcal{M}_X^2}{\mathcal{M}_X^2 + 3},$$

Temp jump

$$\frac{T_2}{T_1} = \frac{5\mathcal{M}_X^4 + 14\mathcal{M}_X^2 - 3}{16\mathcal{M}_X^2},$$

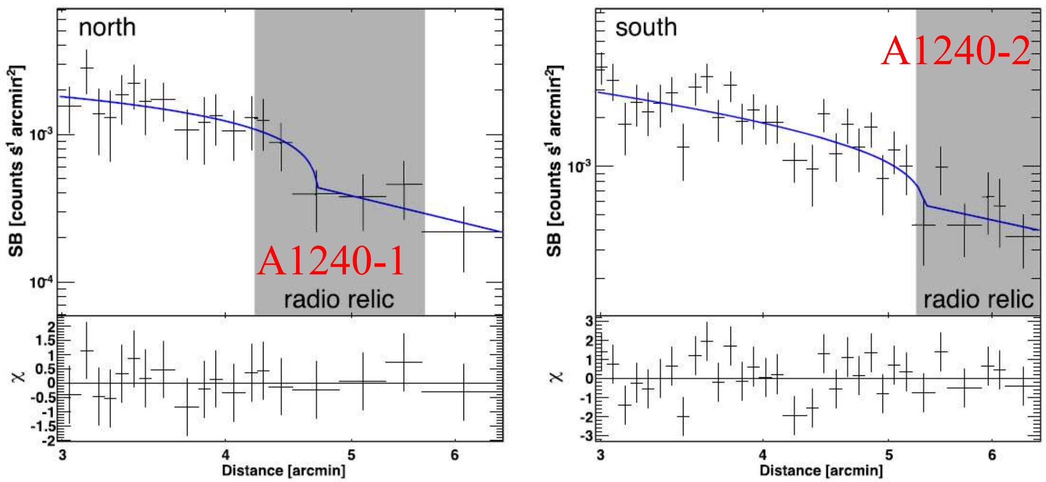

Chandra 0.5–2.0 keV surface brightness

$\rightarrow M_X \sim 2 \leq M_{radio}$

Source	$\mathcal{M}_{int}$	$\mathcal{M}_{inj}$
A1240-1	$5.1^{+3.1}_{-1.1}$	2.4 ± 0.1
A1240-2	$4.0^{+1.1}_{-0.6}$	2.3 ± 0.1
	volume integrated	at shock

Mach Number M_s of Radio Relic Shocks

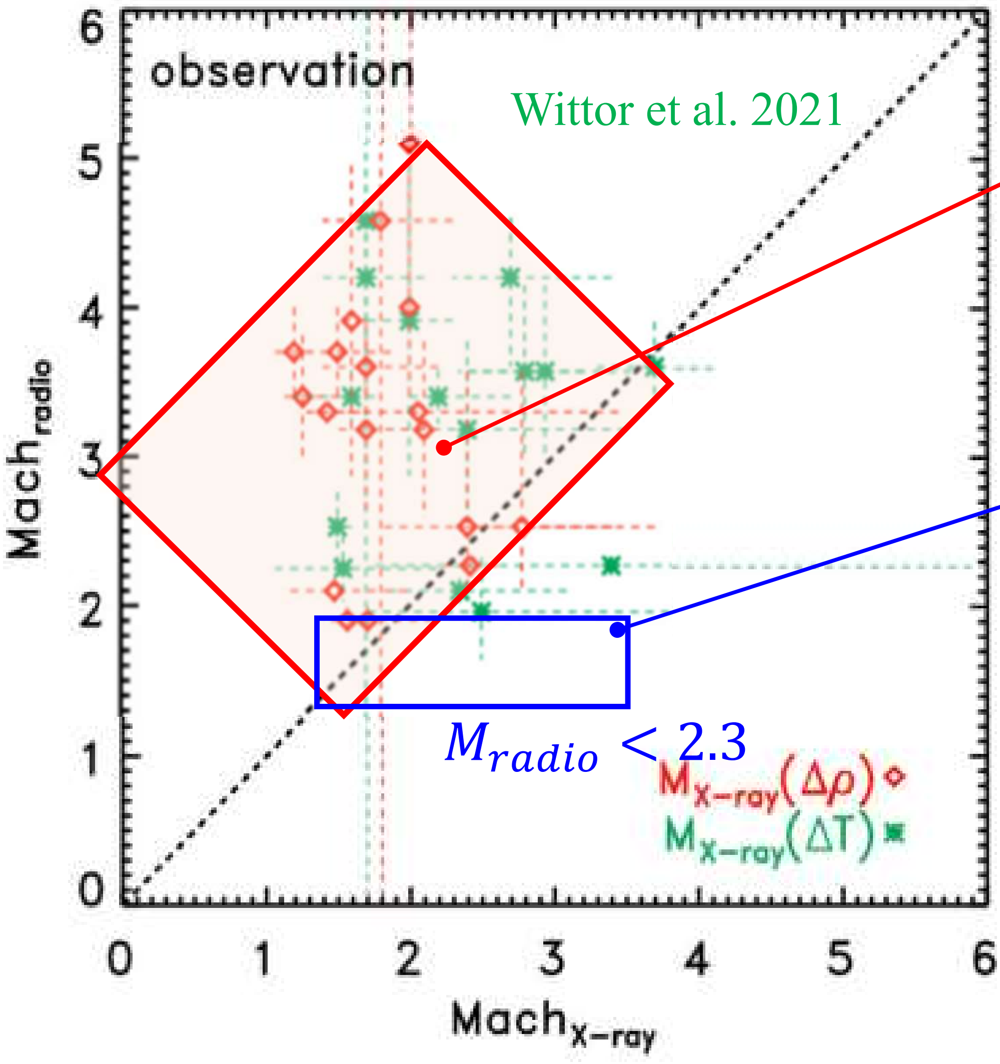

Mach number discrepancy

$$M_{radio} \geq M_X$$

Some observed radio relic shocks seem to have

$M_{radio} < 2.3$ (subcritical)

Q: Are these observations consistent with DSA model?

DSA = Diffusive Shock Acceleration, aka, Fermi first order process.

Shock criticality: subcritical vs. supercritical : ion reflection

Edmiston & Kennel 1984

First fast critical Mach number:

$U_{2x} = c_{s2}$ for ion reflection

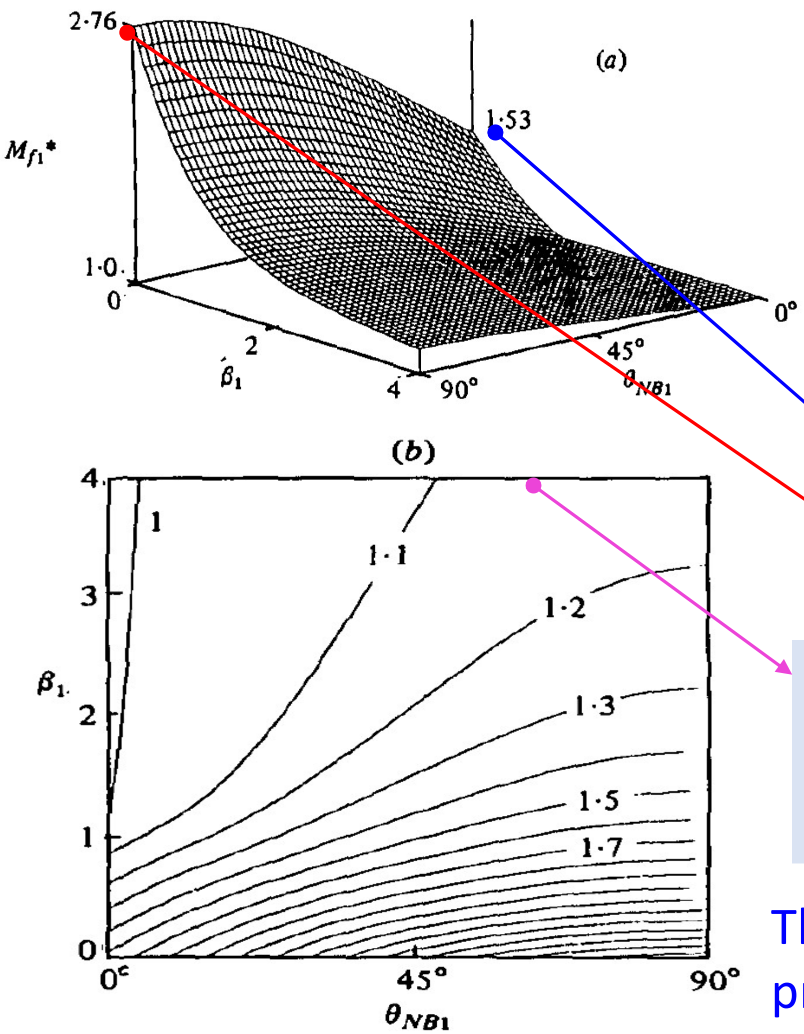

Number flux:

$$N_1 U_{1x} = N_2 U_{2x};$$

Momentum flux:

$$N_1(U_{1x}^2 + V_1^2) + B_{1z}^2/8\pi M = N_2(U_{2x}^2 + V_2^2) + B_{2z}^2/8\pi M,$$

$$B_{1z} B_x/4\pi M = B_{2z} B_x/4\pi M - N_2 U_{2x} U_{2z},$$

$$0 = N_2 U_{2x} U_{2y} - B_x B_{2y}/4\pi M;$$

Energy flux:

$$N_1 U_{1x}(\gamma V_1^2/(\gamma-1) + \tfrac{1}{2}U_{1x}^2) + U_{1z} B_{1z}^2/4\pi M$$
$$= N_2 U_{2x}[\gamma V_2^2/(\gamma-1) + \tfrac{1}{2}U_{2x}^2 + \tfrac{1}{2}U_{2z}^2] + B_{2z}/4\pi M(B_{2z}U_{2x} - B_x U_{2z}).$$

$\beta = 0$ limit — cold plasma

$M_f^* = 1.53$ for $\theta_{Bn} = 0^\circ$ — Parallel shocks

$M_f^* = 2.76$ for $\theta_{Bn} = 90^\circ$ — Perp. shocks

$\beta >> 1$ limit,

$M_f^* \sim 1.0 - 1.1$ for $\theta_{Bn} < 45^\circ$ — $Q_{\parallel}$ shocks

$M_f^* \sim 1.1 - 1.2$ for $\theta_{Bn} > 45^\circ$ — $Q_{\perp}$ shocks

This fluid approach does not account for kinetic processes in the shock transition.

Shock criticality: subcritical vs. supercritical : ion reflection

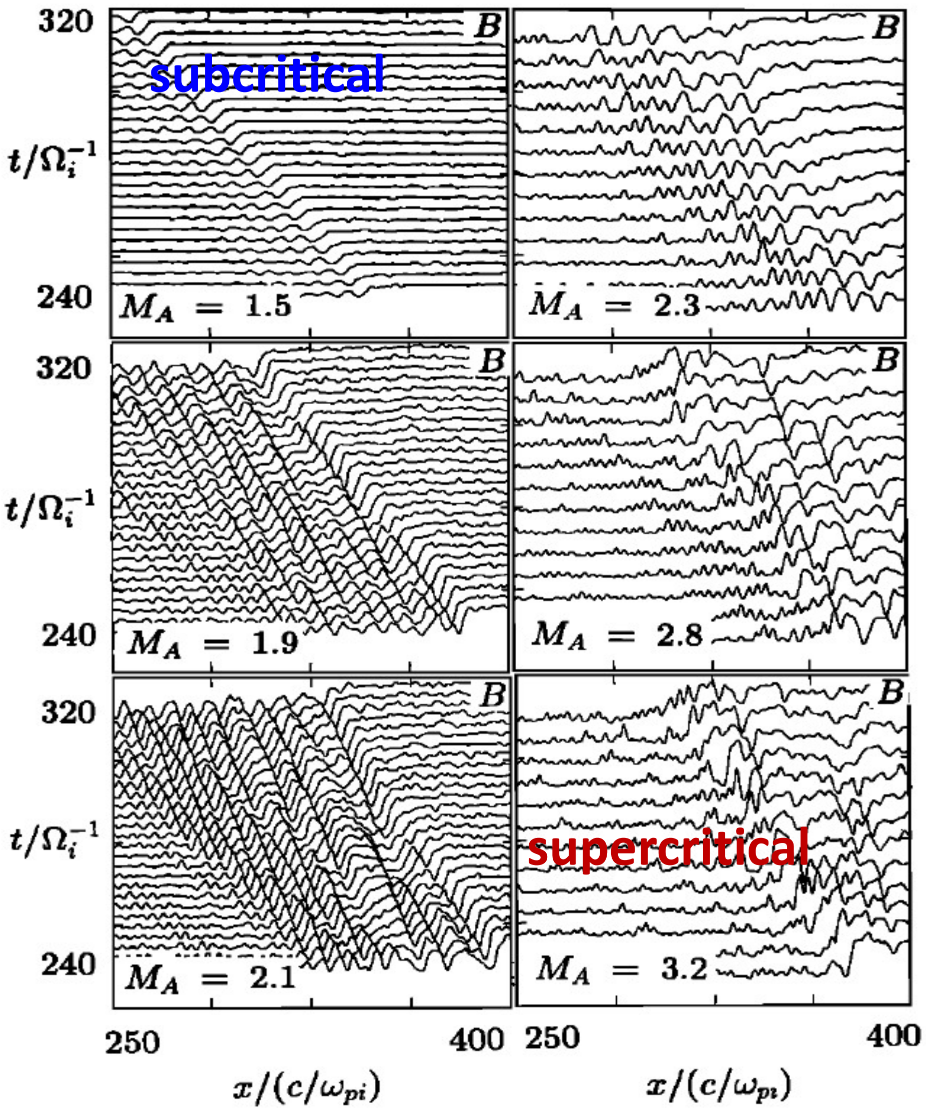

Omidi et el. 1994

1D hybrid simulations: Low M_A $Q_\parallel$ shocks

$$\theta_{Bn} = 30^\circ, \quad \beta_i = 0.5$$

Subcritical shocks:

shock transition is smooth without overshoot/undershoot oscillations.

Supercritical shocks: $M_A > 2.8$

Incoming ions are reflected at shock.

→ Shock is unsteady & undergoes self-reformation.

→ efficient ion reflection

→ lead to "injection" to DSA

Dynamics of reflected ions determine the shock structures.
➔ govern the injection process

Proton injection to DSA: 1D PIC simulations for $Q_{\parallel}$ ICM shocks

Ha, Ryu, Kang + 2018

Table 1. Model Parameters for the Simulations

Model Name[a]	$M_s \approx M_f$	M_A	v_0/c	θ_{Bn}	β	$T_e = T_i$[K(keV)]	$\frac{m_i}{m_e}$
M3.2[d]	3.2	29.2	0.052	13°	100	$10^8(8.6)$	100
M2.0	2.0	18.2	0.027	13°	100	$10^8(8.6)$	100
M2.15	2.15	19.6	0.0297	13°	100	$10^8(8.6)$	100
M2.25	2.25	20.5	0.0315	13°	100	$10^8(8.6)$	100
M2.5	2.5	22.9	0.035	13°	100	$10^8(8.6)$	100
M2.85	2.85	26.0	0.0395	13°	100	$10^8(8.6)$	100
M3.5	3.5	31.9	0.057	13°	100	$10^8(8.6)$	100
M4	4.0	36.5	0.066	13°	100	$10^8(8.6)$	100

Particle in Cell
Both p + e are kinetic.

Weak $Q_{\parallel}$ shocks

in β=100 ICM

M_s= 2.0 - 4.0

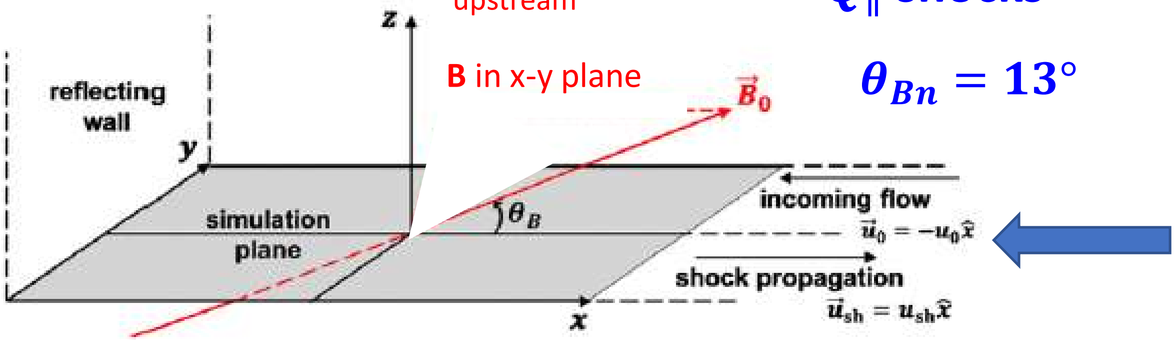

$Q_{\parallel}$ shocks

$\theta_{Bn} = 13°$

shock parameters
$M_s = U_s/c_s$
$M_A = U_s/V_A$
$M_A \approx \beta_p^{1/2} M_s$
$\beta_p = P_{gas}/P_B$
$= nkT/(B^2/8\pi)$
θ_{Bn} : obliquity angle

Incoming plasma is reflected at the wall.

A shock propagates into the incoming flow.

Proton injection to DSA: 1D PIC simulations for $Q_{\parallel}$ shocks

Ha et al. 2018

$\theta_{Bn} = 13°$ $\beta = 100$

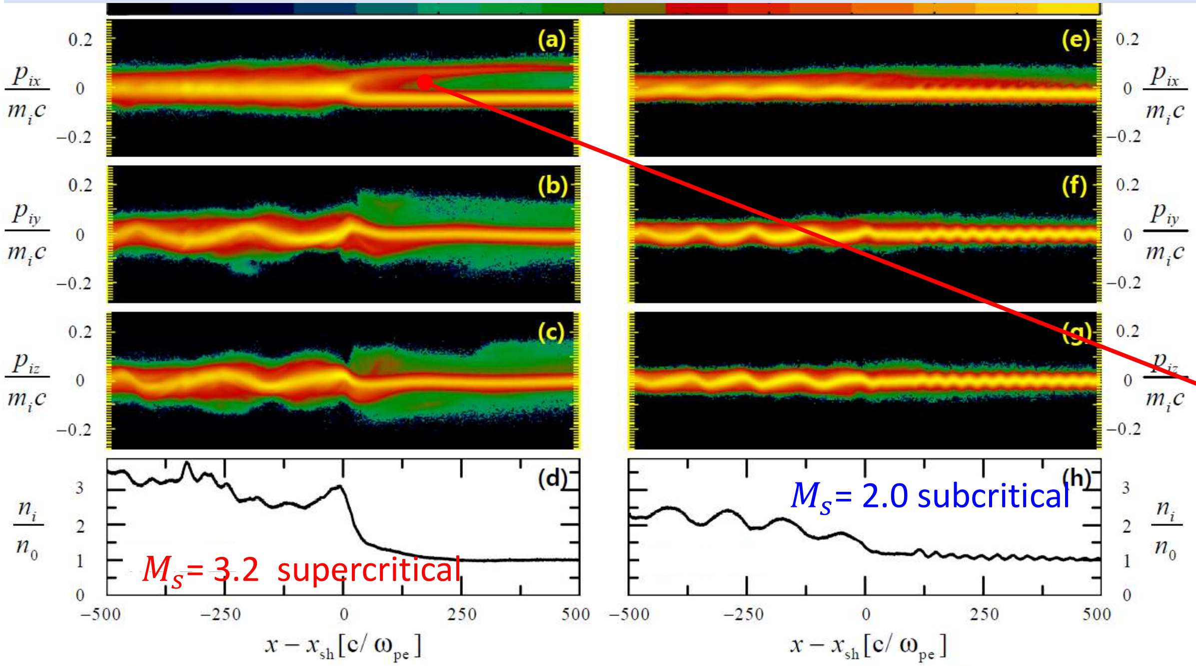

Dynamics of reflected ions
→ determines shock structure
→ forms suprathermal tail
→ leads to Proton injection to DSA

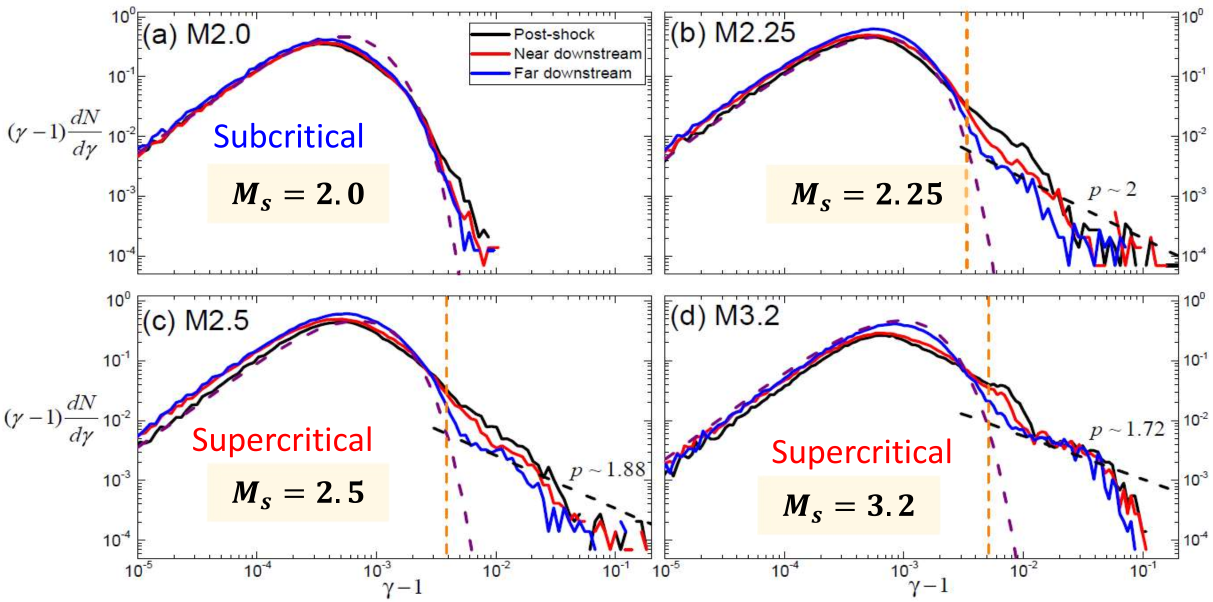

Mach number dependence
→$M_{crit} \sim 2.3$

In high β ICM, only supercritical $Q_{\parallel}$ shocks with $M_s \geq 2.3$ may inject and accelerate CR protons via DSA.

Electron preacceleration in weak high-β $Q_\perp$ ICM shocks

Guo et al. 2014a,b

$$\beta = \frac{P_{gas}}{P_B} \sim 20$$

$$(6 - 200)$$

$$M_s = 3.0$$

$$\theta_{Bn} = 13 - 80°$$

1. reflection by magnetic deflection (mirror) at the shock ramp
2. Shock Drift Acceleration (SDA) along the shock surface
3. backstreaming electrons generates T anisotropy ($T_{e_\parallel} > T_{e\perp}$)
4. Electron Firehose Instability (EFI) excites obliques waves
5. undergo Fermi-like acceleration in the upstream region

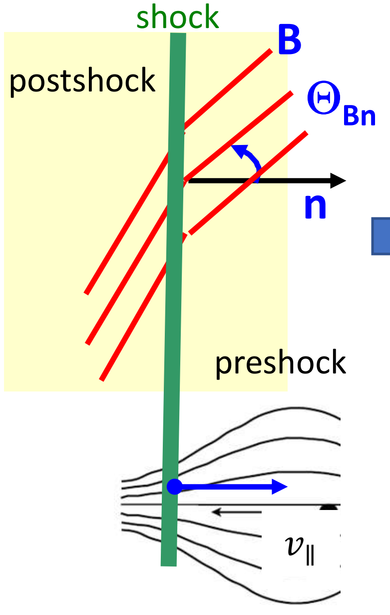

magnetic mirror reflection

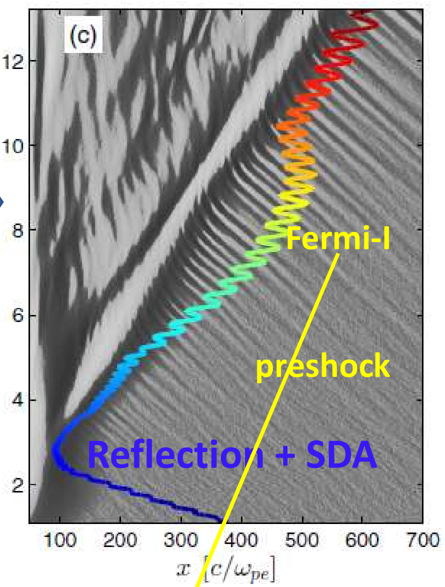

electron trajectory

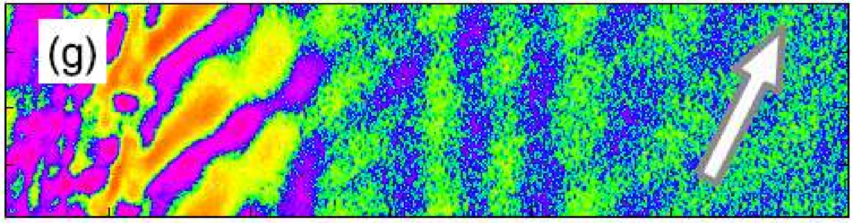

EFI-induced oblique waves in preshock region

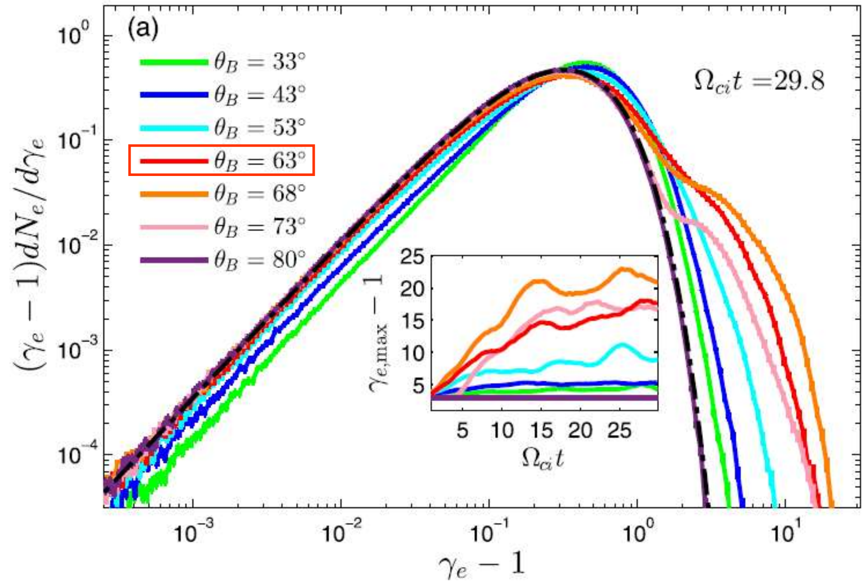

Fermi-like acceleration due to scattering btw the shock and upstream waves.

Kang + 2019

2D PIC simulations for $Q_\perp$ ICM shocks for electron pre-acceleration

Model Name[a]	M_s	M_A	v_0/c	θ_{Bn}	β	$T_e = T_i$[K(keV)]	$\frac{m_i}{m_e}$
M2.3[d]	2.3	21	0.0325	63°	100	$10^8(8.6)$	100
M2.0	2.0	18.2	0.027	63°	100	$10^8(8.6)$	100
M2.15	2.15	19.6	0.0297	63°	100	$10^8(8.6)$	100
M2.5	2.5	22.9	0.035	63°	100	$10^8(8.6)$	100
M2.75	2.75	25.1	0.041	63°	100	$10^8(8.6)$	100
M3.0	3.0	27.4	0.047	63°	100	$10^8(8.6)$	100

$$\beta = \frac{P_{gas}}{P_B} = 100$$

$$\theta_{Bn} = 63°$$

$$M_s = 2.0 - 3.0$$

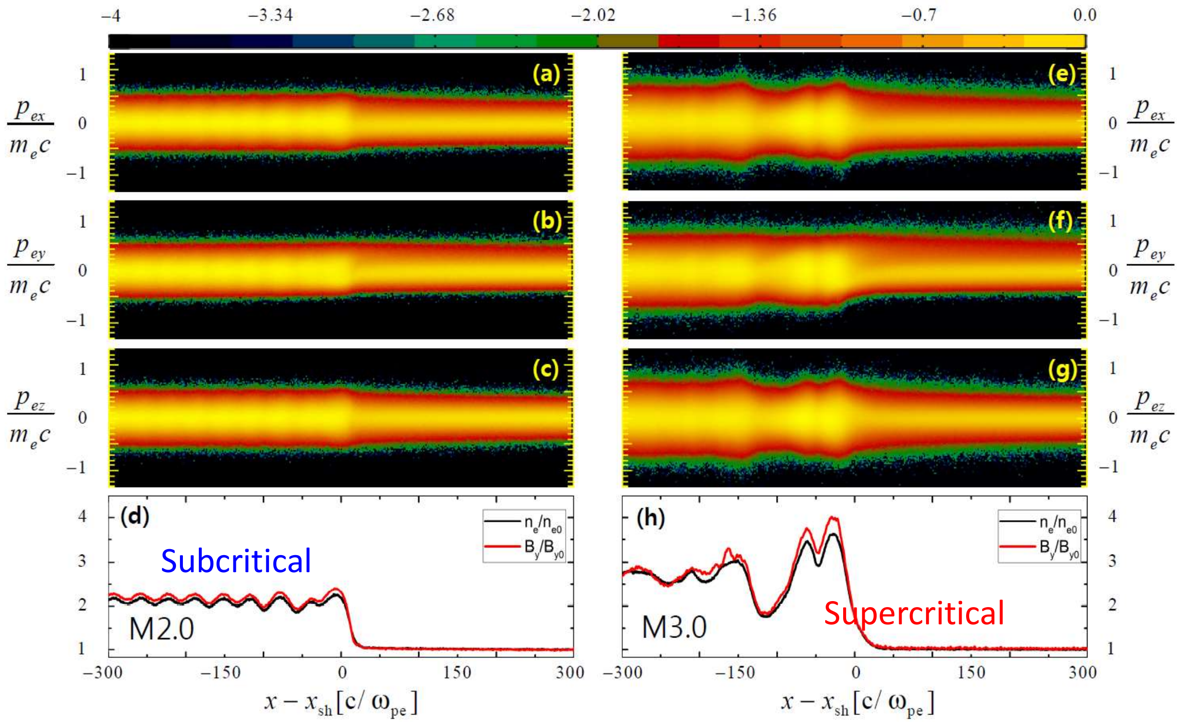

Similarly as in $Q_\parallel$ shocks, dynamics of reflected ions determines the shock structure of $Q_\perp$ shocks.

Kang + 2019

Shock Criticality: dynamics of reflected ions→ electron reflection

Fraction of reflected ions

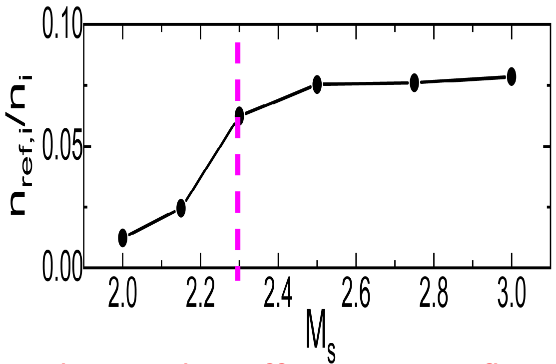

subcritical: inefficient ion reflection

supercritical: efficient ion reflection

Shock structure

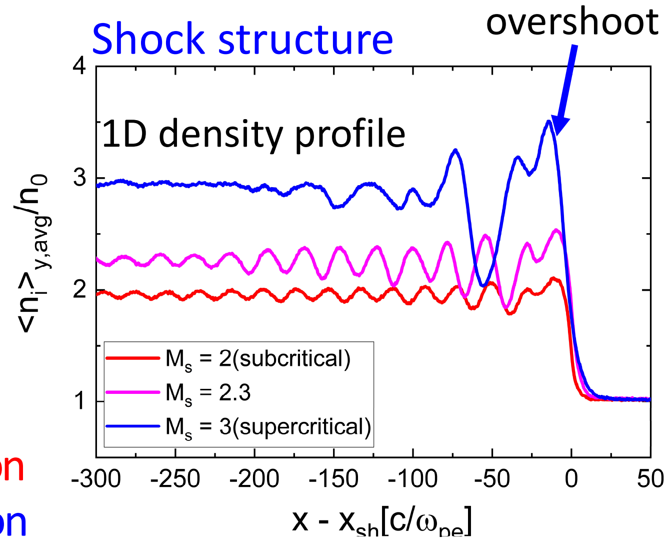

EFI instability parameter

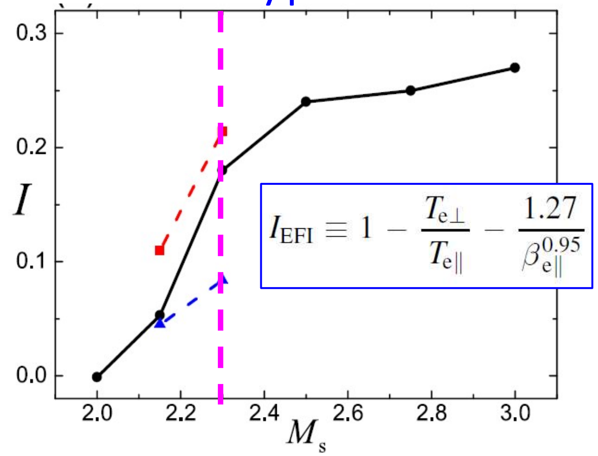

$M^*_{EFI} \sim 2.3$: critical Mach number for the EFI excitation

Upstream waves

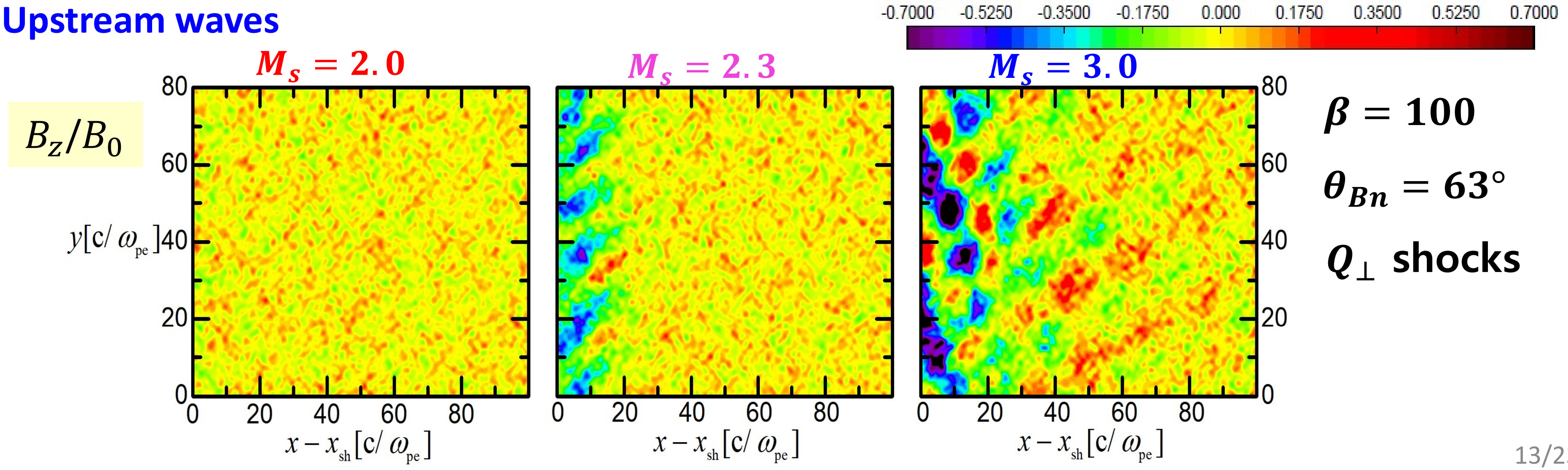

$\beta = 100$

$\theta_{Bn} = 63°$

$Q_\perp$ shocks

2D PIC simulations for $Q_\perp$ shocks : electron pre-acceleration

Kang + 2019

$\beta \sim 100$

$M_s = 2.0 - 3.0$

Blue: $\Omega_{ci}t = 10$, Red: $\Omega_{ci}t = 30$, Green: $\Omega_{ci}t = 60$

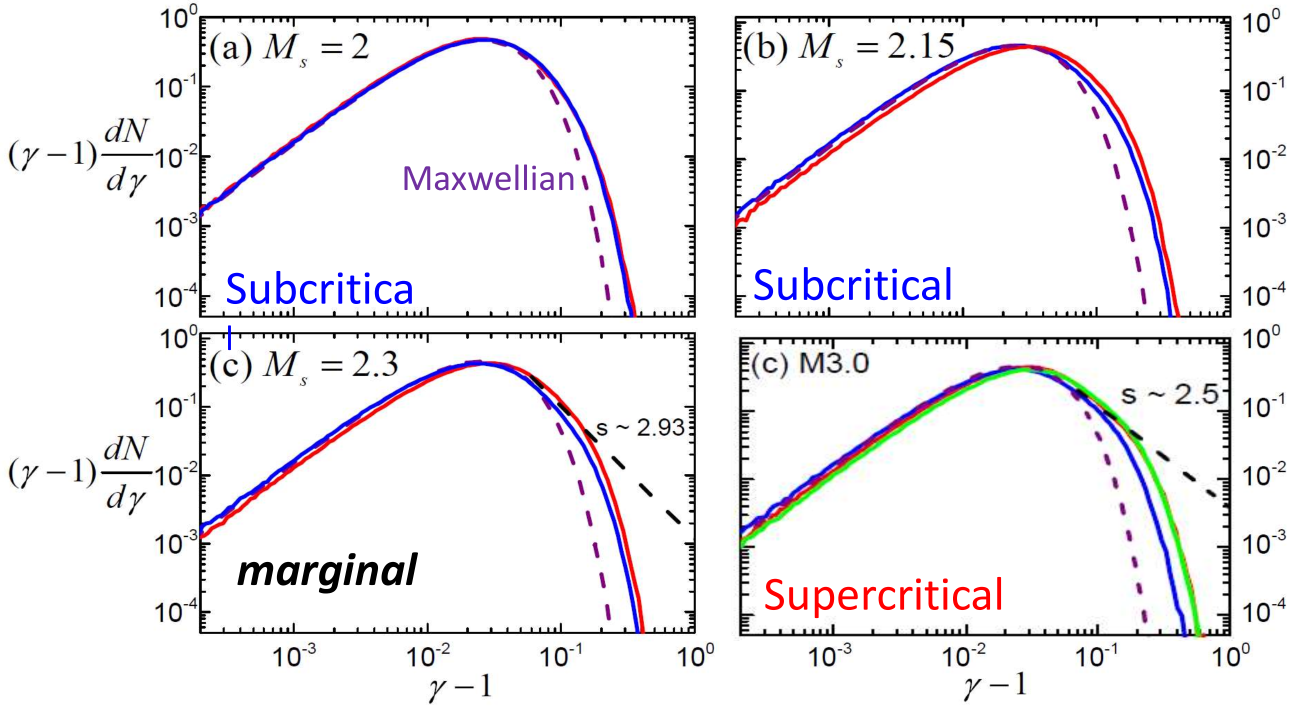

-**Subcritical shocks:** only single SDA cycle (no Fermi-I)

-**Supercritical shocks:** multiple cycles of SDA due to scattering off upstream waves

→ suprathermal tail develops via Fermi-like acceleration

-But pre-acceleration is saturated due to lack of powers in longer λ waves in these simulations

➔ Much larger simulation box (in y-direction) is necessary to capture ion-scale waves due to shock surface rippling is necessary.

Electron acceleration at quasi-perp shocks in sub- and supercritical regimes: 2D and 3D simulations

$\beta_i \approx \beta_e \approx 0.5$ **Hybrid sim.** + test-particle electron

Trotta & Burgess 2019

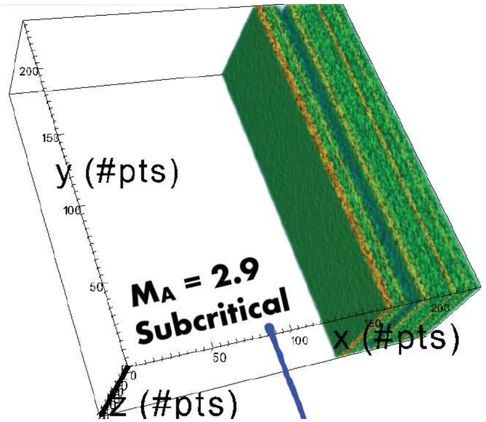

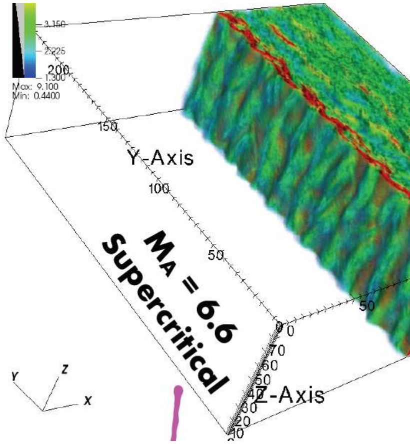

rippling

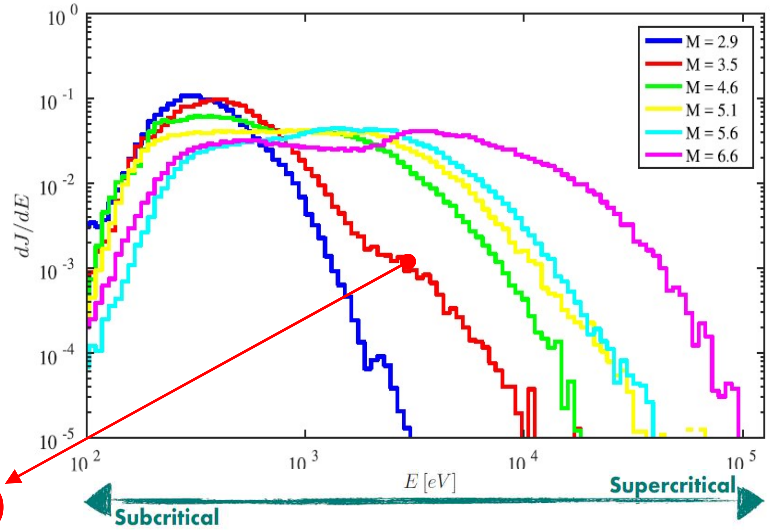

Supercritcal shocks ($M_A > 3.5$)

Electron Acceleration at Rippled Low-Mac-Number Shocks in High-Beta Collisionless Cosmic Plasmas

$\beta = 5\ (\beta_e = \beta_i = 2.5)$ 2D PIC

Niemiec + 2019, Kobzar + 2021

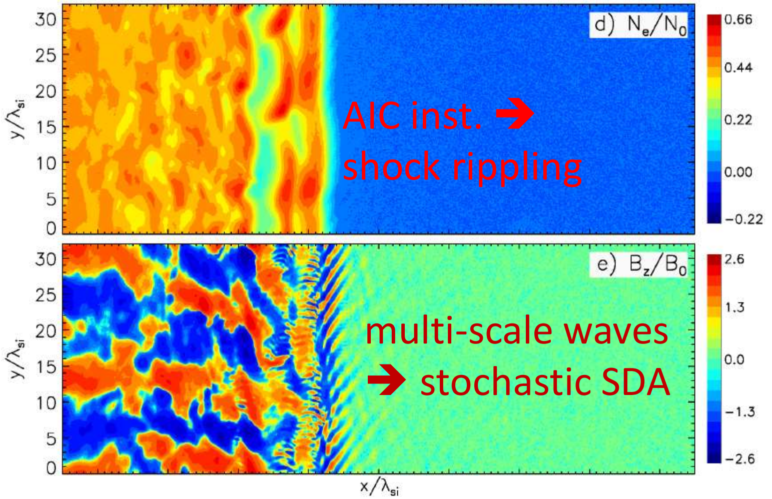

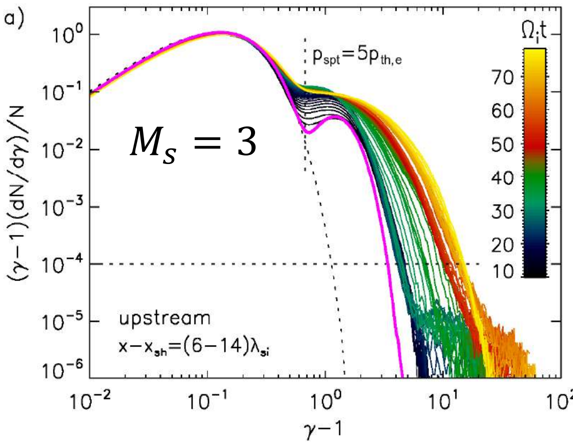

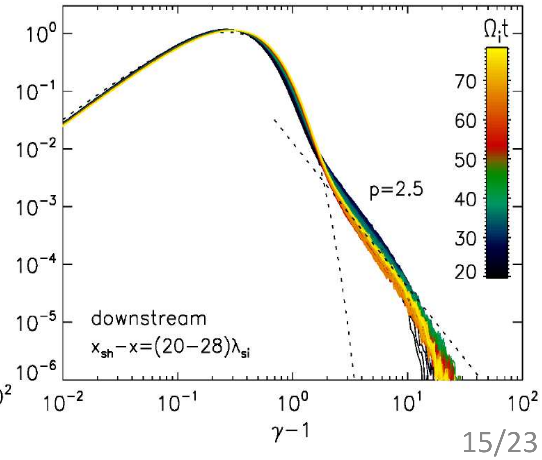

Alfven ion cyclotron (**AIC**)

Structure of supercritical $Q_\perp$ shocks

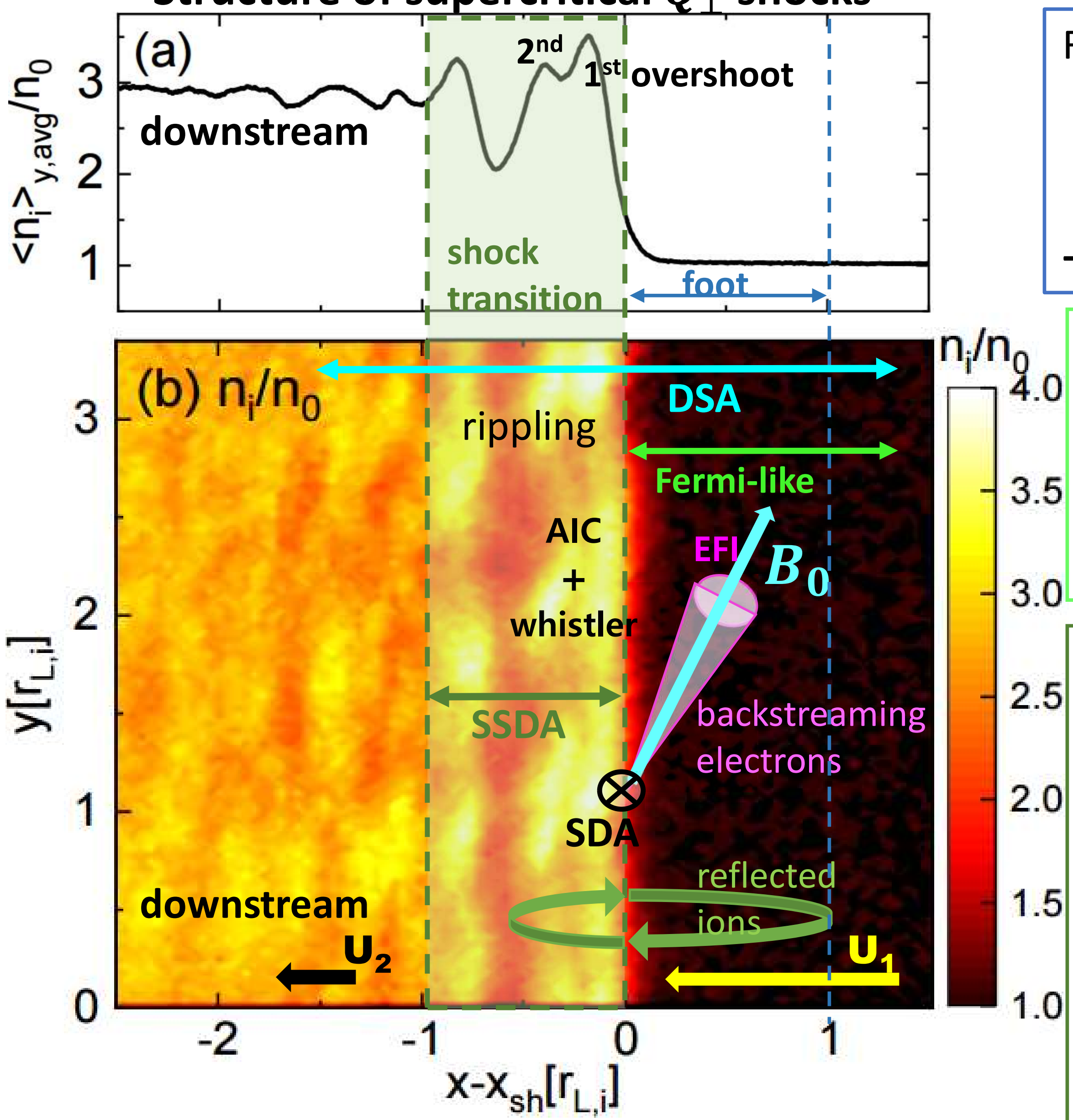

(Guo + 2014, 2017; Katou & Amano 2019; Kobzar + 2021)

Microinstabilities

Kim + 2021

Free energy source:
- temperature anisotropies

$$\frac{T_{\perp a}}{T_{\parallel a}} > 1, \quad \frac{T_{\parallel a}}{T_{\perp a}} > 1$$

- due to beams of reflected ions/electrons

➢ In the shock upstream

$\frac{T_{\parallel e}}{T_{\perp e}} > 1$ electron firehose instability (EFI)

➔ Fermi-like acceleration

➢ In the shock transition zone

$\frac{T_{\perp e}}{T_{\parallel e}} > 1$
1. whistler instability (WI)
2. electron mirror instability

$\frac{T_{\perp i}}{T_{\parallel i}} > 1$
1. Alfven ion cyclotron (AIC)
2. ion mirror instability

➔ Stochastic SDA

Electron Preacceleration at Weak $Q_\perp$ ICM Shocks: Effects of Shock Surface Rippling

PIC simulations in Kang + 2019 $\beta = 100$; $\theta_{Bn} = 63°$; $M_s = 2.0 - 3.0$; $\frac{m_i}{m_e} = 100$

➔ 2D simulation domain is increased 5 times in y-direction to include ion-scale instability.

Model Name	M_s	M_A	u_0/c	θ_{Bn}	β	$T_{e0} = T_{i0}$ [K(keV)]	m_i/m_e
M2.0	2.0	12.9	0.038	63°	50	10^8 (8.6)	50
M2.15	2.15	13.9	0.042	63°	50	10^8 (8.6)	50
M2.3	2.3	14.8	0.046	63°	50	10^8 (8.6)	50
M2.5	2.5	16.1	0.053	63°	50	10^8 (8.6)	50
M2.8	2.8	18.1	0.061	63°	50	10^8 (8.6)	50
M3.0	3.0	19.4	0.068	63°	50	10^8 (8.6)	50

$\beta = 50$

$\frac{m_i}{m_e} = 50$

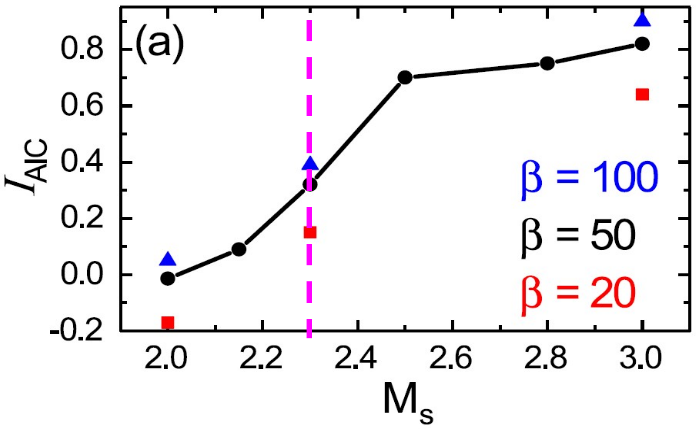

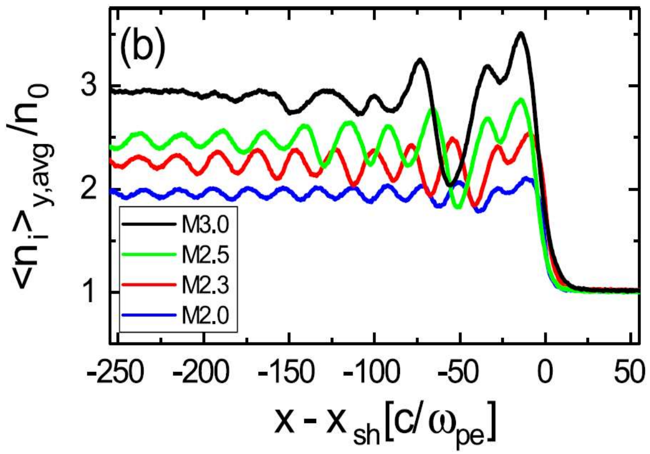

$M^*_{AIC} \sim 2.3$: critical Mach number for the AIC excitation. Also governed by the dynamics of reflected ions.

$$I_{AIC} = \frac{T_{i\perp}}{T_{i\parallel}} - 1 - \frac{S_p}{\beta_{i\parallel}^{\alpha_p}} > 0$$

(Gary + 1997)

*Alfven ion cyclotron (AIC)

Electron Preacceleration at Weak $Q_\perp$ ICM Shocks: Effects of Shock Surface Rippling

2D PIC simulations with a larger simulation box

Kang + 2019 vs. Ha + 2021

$$\frac{m_i}{m_e} = 50, T = 10^8 K, \beta = 50, M_s = 2-3,\ \theta_{Bn} = 63^\circ$$

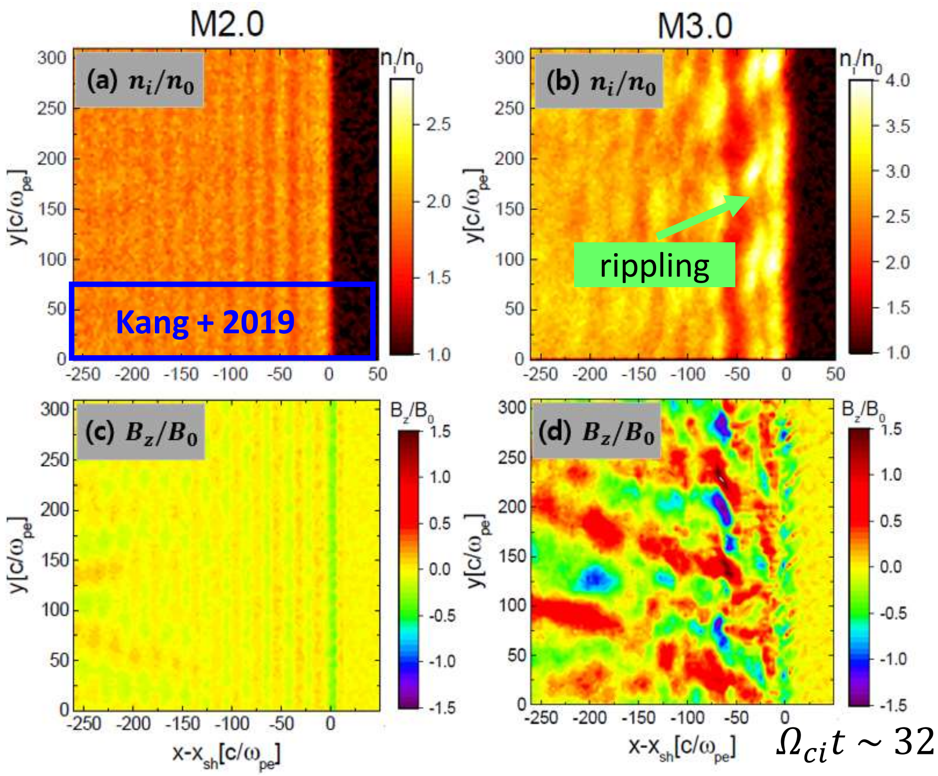

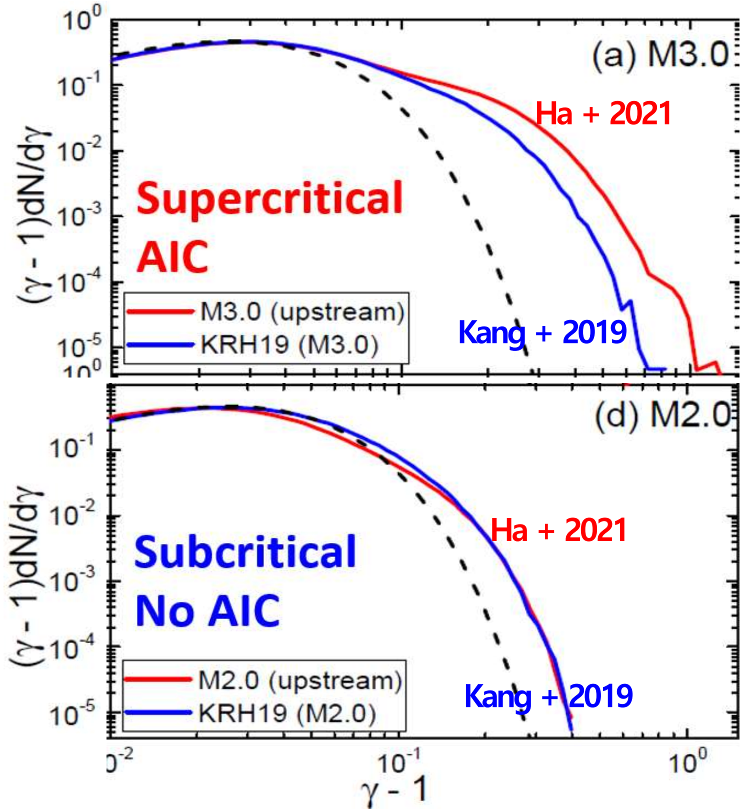

In supercritical shocks with $M_s > 2.3$,
ion temperature anisotropy ($T_{i\perp}/T_{i\parallel} > 1$) due to shock-reflected ions → trigger **the AIC instability**

*Alfven ion cyclotron (AIC)

→ shock surface rippling → multi-scale waves longer than electron-scales
→ extended SDA (so-called **Stochastic SDA,** Katou & Amano 2019)

But electron injection/acceleration at subcritical shocks ($M_s < 2.3$) remains unknown.

Mach Number M_s of Radio Relic Shocks

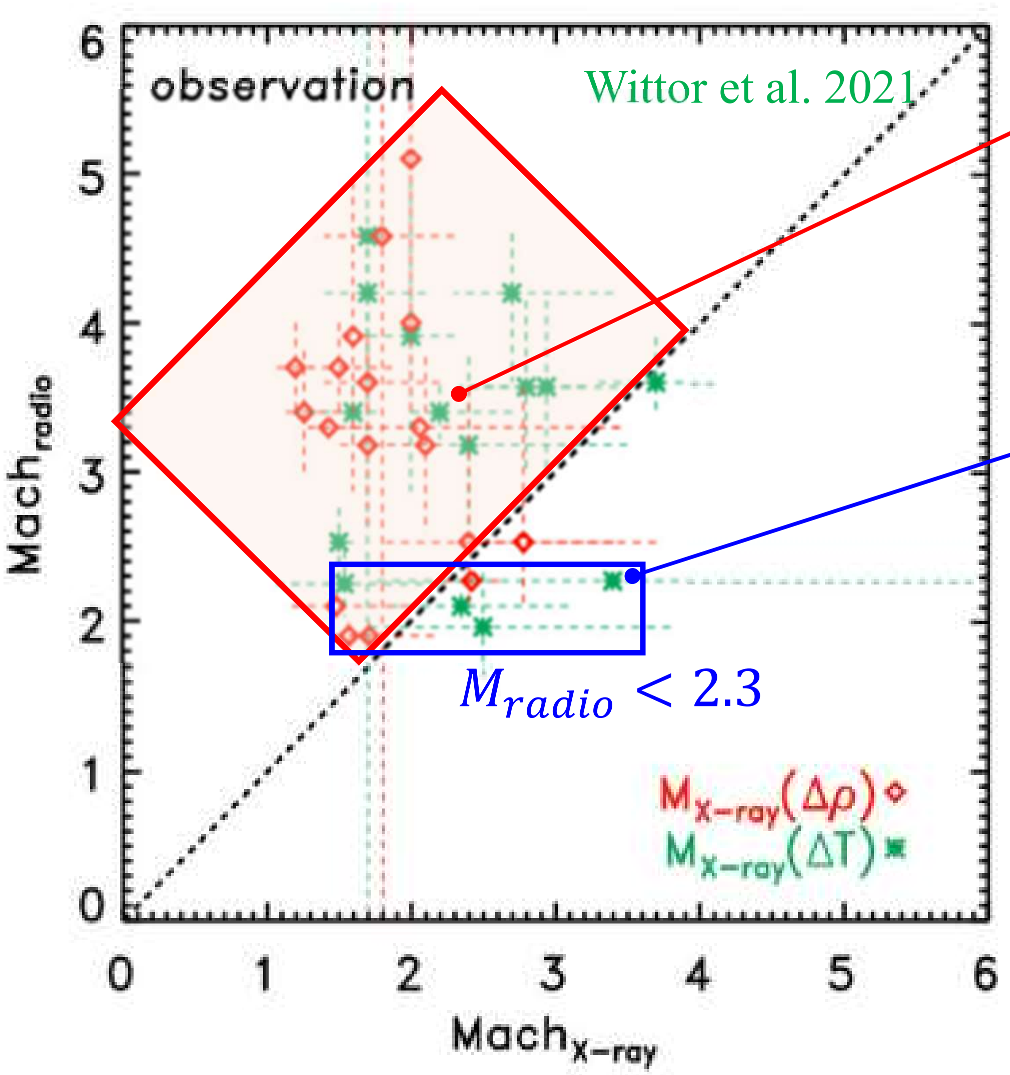

Mach number discrepancy

$$M_{radio} \geq M_X$$

Some observed radio relic shocks seem to have

$M_{radio} < 2.3$ (subcritical)

Q: Are these observations consistent with DSA model?

Re-acceleration of fossil CR electrons

Some puzzles in DSA model with *in situ* injection only

(1) Injection & DSA may be inefficient at subcritical shocks ($M_s < 2.3$).

(2) For some radio relics, $M_{\rm radio} > M_{\rm X}$ i.e., radio spectral index is flatter than expected.

(3) Some X-ray shocks do not have associated radio relics ($Q_{\parallel}$ shocks?).

(4) Only ~10 % of merging clusters host radio relics, while numerous shocks are expected to form in ICM ($Q_{\parallel}$: $Q_{\perp}$ = 1: 3 for turbulent B fields).

Possible solution is Re-acceleration model:
a radio relic forms when a weak shock encounters the ICM plasma with pre-existing fossil electrons.

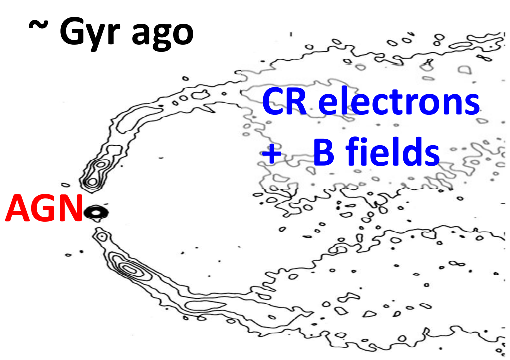

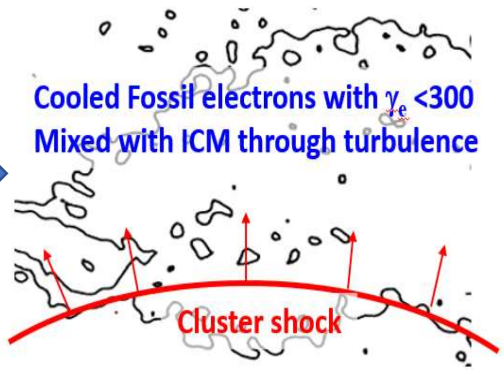

Birth of a radio relic

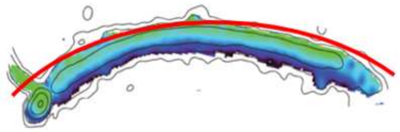

Subcritical shocks with $M_s < 2.3$ possible?

(Kang + 2012, Kang 2016, Pinzke + 2013)

"Electron Preacceleration at subcritical $Q_\perp$ ICM Shocks: Effects of Pre-existing Suprathermal Electrons"

Ha et al. 2022

2D PIC simulations:
suprathermal electrons added to incoming thermal plasma

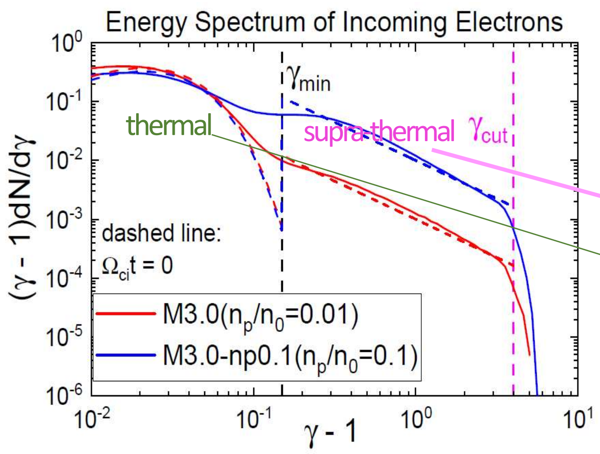

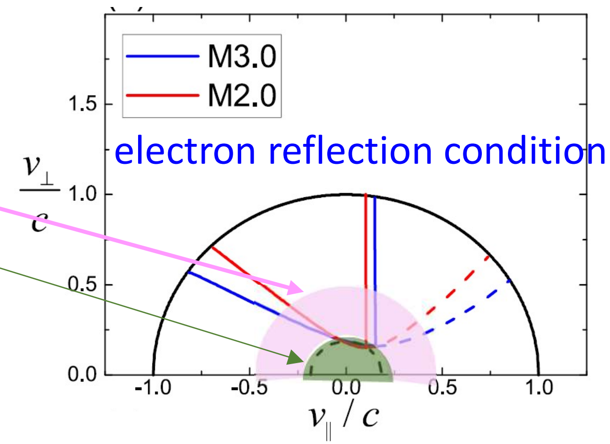

Reflection fraction

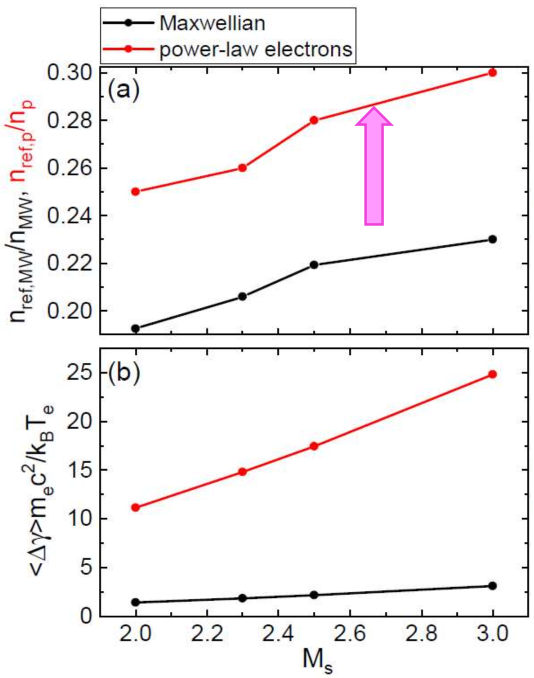

T anisotropies

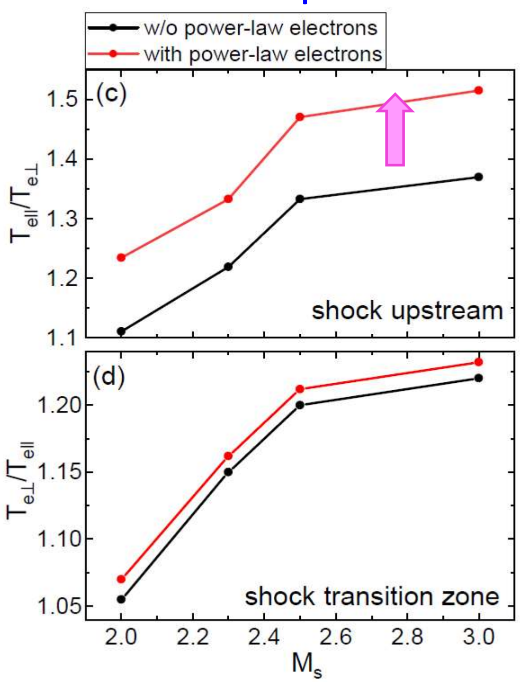

Instability parameter

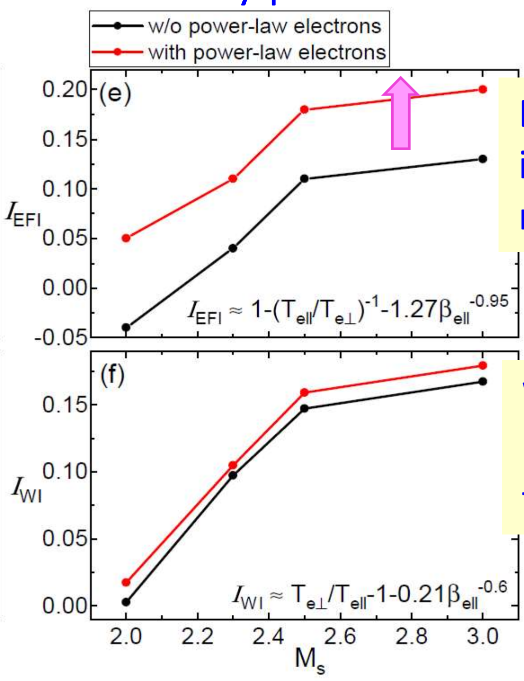

EFI is enhanced in the upstream region.

WI is enhanced in the shock transition.

"Electron Preacceleration at subcritical $Q_\perp$ ICM Shocks: Effects of Pre-existing Suprathermal Electrons"

Ha et al. 2022

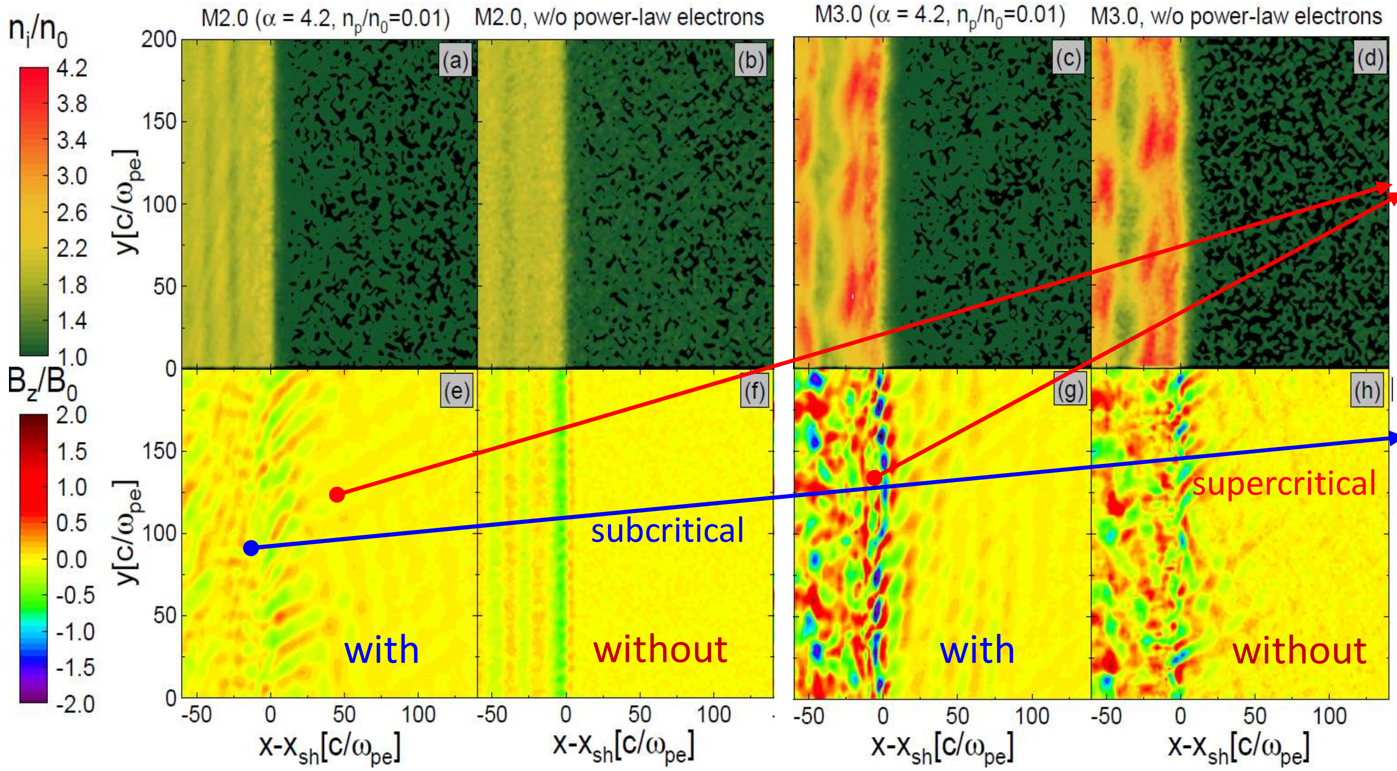

Effects of pre-existing suprathermal Electrons : → enhance EFI & WI waves

No AIC (shock surface rippling) is excited at subcritical shocks

Pre-existing nonthermal electrons do not enhance ion-scale waves
→ Electron injection to DSA remains inefficient at subcritical shocks.

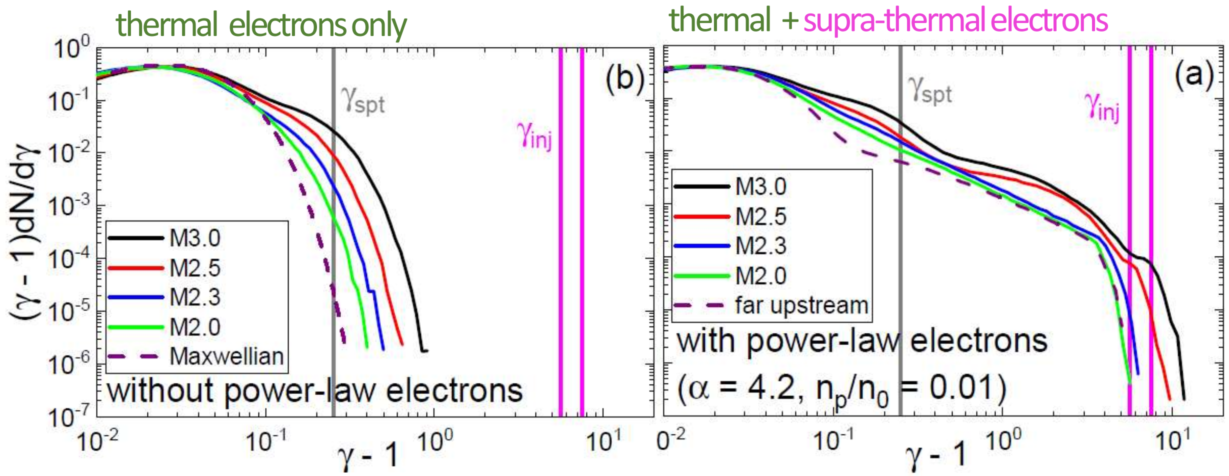

The origin of radio relics with $M_s < 2.3$ requires extra ingredients such as pre-existing turbulence on kinetic ion scales.

Summary: Take Home Messages

1. In high β ICM, only supercritical $Q_{\parallel}$ shocks with $M_s > 2.3$ may inject suprathermal protons to DSA and produce CR protons (Ha + 2018, Ryu + 2019).

2. Ion-scale shock surface rippling at supercritical $Q_{\perp}$ shocks with $M_s > 2.3$ may generate multi-scale waves, leading to the electron injection all the way to DSA in high β shocks. (e.g. Katou & Amano 2019, Trotta & Burgess 2019, Niemiec + 2019, Ha + 2021, Kobzar+2021).

3. Pre-existing nonthermal electrons at weak $Q_{\perp}$ shocks can enhance the excitation of the EFI & WI, but not the AIC instability.

➔ So ion scale waves are not generated and electron pre-acceleration remains ineffective at subcritical shocks. (Ha + 2022)

4. Outstanding question: Can subcritical shocks (M_s< 2.3) (re)-accelerate electrons ($Q_{\perp}$ shocks) in the presence of pre-existing turbulence on kinetic scales in the upstream region ? (e.g. Giacalone 2005; Guo & Giacalone 2015)

Observed Radio relics have $M_s \sim 1.5 - 3.0$